Pad-Printed Prussian Blue doped carbon ink for real-time peroxide sensing in cell culture

Craig McBeth[1,*] Craig.McBeth@Warwick.ac.uk, Andrew Paterson[2], Duncan Sharp[2]
[1]School of life sciences, faculty of science, The University of Warwick, Coventry, UK.

[2]Centre for Biomedical Science Research, School of Clinical and Applied Sciences, Leeds Beckett University, Leeds, UK

[*]**Corresponding author at:** The University of Warwick

Abstract

Hydrogen peroxide has important roles within cellular functions, as a prevalent form of Reactive Oxygen Species, detection within mammalian cells is of metabolic importance; typically requiring cell lysis or fluorescence-based methods to quantify.

Herein, we explore the novel use of Prussian blue mediated, pad printed carbon electrodes to allow the indirect detection of cellular peroxides in bulk culture media, which facilitates non-invasive, real-time detection.

Electrodes demonstrated capacity to detect H_2O_2 with a linear range of 1-200µM in CMEM (R^2 =0.9988), enabling detection of peroxides found in culture media and lysate. Developed electrodes had a Limit of Detection (LOD) of 0.4µM H_2O_2 in Britton-Robinson Buffer (BRB), 0.38µM in Eagle's Minimum Essential Medium (EMEM) and 9.19 µM in Dulbecco's Modified Eagles Medium (DMEM). Electrodes were tested in a conventional 5% serum supplemented EMEM (CMEM) and demonstrated an LOD of 0.5µM and LOQ of 0.9µM.

The results demonstrate proof of concept for monitoring H_2O_2 in complex culture media with potential long-term use and reusability using simple, pad printed Prussian Blue / Carbon electrodes. The lack of further modification, and cost-effectiveness of these disposable electrodes could offer great advancement to monitoring of peroxides in complex media.

Key Words: Prussian blue; cell culture; pad-printed carbon electrodes; bulk analysis; hydrogen peroxide.

1. Introduction

Hydrogen peroxide (H_2O_2) has well-established roles in cell signalling[1] and cell death[2]; its presence can be an indicator of intracellular and extracellular responses to potentially damaging stimuli, such as direct or indirect reactive oxygen species (ROS) inducing agents[3]. In biological systems, H_2O_2 is utilised and generated through several biochemical reactions, such as those catalysed by oxidase enzymes and superoxide dismutases, and as such are a vital component of cell metabolism[1]. Whilst H_2O_2 is necessary for cellular function, fluctuations in concentration can induce cell dysfunction, upregulate the antioxidant response of the cell and/ or cause cell death/ mutation[4].

As such, the ability to detect H_2O_2 continuously in real-time within cell culture media holds significance for academic, industrial, and pharmacological application/ purposes[5]. Electrochemical methods using non-modified metal electrodes for the measurement of H_2O_2 are limited by the high over-potential required for oxidation (~0.7V versus Ag/AgCl), and several biologically relevant electroactive substances, such as glucose, ascorbic acid, uric acid, tryptophan and tyrosine are typically oxidised at similar potentials.

Whilst the measurement of H_2O_2 itself is well established as a fundamental unpinning of many biosensors either as analytical target or product of an immobilised enzyme, they still require mediating compounds to effectively shuttle electrons. A challenge to using enzyme-based biosensors arises due to potential issues with stability, complexity and cost. Therefore, the use of non-enzymatic methods for electrochemical detection of hydrogen peroxide is particularly advantageous and has been previously facilitated through a range of electrode modifiers, such as: metal hexacyanoferrates (e.g. iron , copper, nickel, cobalt, chromium, vanadium, manganese and ruthenium[6,7]), carbon nanotubes and graphene[8–12], and various nanoparticles (e.g. AgO, ZnO,Fe_3O_4 and CuO[13–16]).

Prussian Blue (PB) and its analogues have commonly been exploited to allow peroxide sensing through deposition onto various carbon electrode surfaces via electropolymerisation in a highly concentrated acidic solution (such as H_2SO_4 or HCl) or drop casting[17]. Reduced PB is capable of reducing H_2O_2 to various forms, literature cites either hydroxyl ions, water or a combination. This process oxidises PB, which is then in turn reduced by the electrode, mechanism shown in Figure 1.

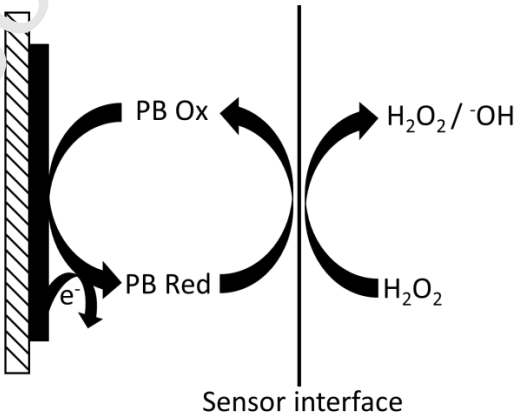

Figure 1. PB redox cycling through the reduction of H_2O_2 to form H_2O_2 and/or ^{-}OH.

Though PB can be polymerised or solvent cast onto the electrode surface easily, desorption occurs rapidly and therefore requires binding agents/ co-polymers to assist with electrode

adhesion[18]. Hence, the semi-conductive polymer poly(*O*-phenylenediamine)(PoPD) has been widely used as a supporting polymer[19], as has Nafion[20], and pyrrole[21].

However, due to the increase in popularity of printed electrodes, ink/paste formulations with incorporated mediators have previously been developed with results comparable to modified electrodes[22]. Prussian blue has widespread use in H_2O_2 sensing with a redox window between -0.2 to 0.4V, with several studies utilising ~0.0V for amperometric measurements[20,23,24].

H_2O_2 detection via PB has been utilised in combination with additional modifiers in an attempt to enhance sensitivity and selectivity towards H_2O_2, including pyrrole[25], Single-walled carbon nanotubes (SWCNTs)[26], Multi-walled carbon nanotubes (MWCNTs)[27], nanoparticles[28], and various polymers[18]. Commonly, modifiers are utilised to form polymers or as a supporting matrix for PB, deposited onto the electrode surface through electropolymerisation or solvent evaporation.

Table 1 outlines a selection of carbon electrodes modified with PB for H_2O_2 detection. Linear ranges vary between electrodes, with most demonstrating a limit of detection (LOD) of ~0.1-1.0µM and a limit of quantification (LOQ) of ~0.5-2 µM. This sensitivity illustrates the potential for this sensing approach to be developed towards the detection of low concentrations of H_2O_2 released from cells into the surrounding medium – either through cell lysates or bulk culture media analysis (i.e. without sampling or preparation).

Table 1 – Prussian blue modified carbon electrodes capable of H_2O_2 detection.

Working electrode	Linear range	LOD	Medium (pH)	References
GCE	0.1µM-10mM	0.1µM	0.1M HCl + KCl (-)	29
	-	-	PBS (7.3)	30
	0.08-1.0mM	0.04mM	PBS (6.0)	31
	1-800 µM	0.5µM	PBS (6.5)	32
GCE + PEDOT	0.5–839 µM	0.16 µM	PBS (5.7)	33
GCE + PANI-HNT	4-1064 µM	0.226 µM	PBS (7.0)	34
GCE/PB/MoS_2-rGO	0.3 µM-1.5mM	0.14µM	PBS (6.0)	35
GCE/PBMCs/g-CNTs	25nM-1.5mM	13nM	PBS (6.8)	36
Carbon fibre	-	0.1–0.4µM	PBS (7.4)	37
Graphite	0-4.5mM	0.2µM	PBS + 0.1M KCl (7.4)	38
Graphite SPEs	1-500 µM	1µM	PBS + 0.1M KCl (7.4)	39
Carbon paste	2.5-2000µM	2.5µM	PBS (6.0)	40
Carbon nanotube paste	50-5000nM	4.74nM	PBS (7.0)	41
Carbon graphite ink	1-4500 µM	0.1µM	PBS (-)	42
SPCE	0.4-100µM	0.4µM	PBS (7.4)	24
	20-700 µM	20µM	PBS (6.6)	43

g-CNTs: graphenated-carbon nanotubes; **GCE:** glassy carbon electrode; **MPS**: (3-Mercaptopropyl)-trimethoxysilane; **PANI-HNT:** polyaniline coated-halloysite nanotubes; **PBMCs**: Prussian blue microcubes; **rGO**: reduced graphene oxide; **SPE:** screen printed electrode; **SPCE**: screen printed carbon electrode

Bulk analysis of culture media would allow for the non-invasive detection of specific markers associated to changes in cellular behaviour/ metabolism. Hence, a system with the sensitivity to detect these small changes *in-situ* would be advantages in long term monitoring of cell metabolism. The bulk solution, in this context, relates to the whole aqueous

environment that both supplies the cells with essential nutrition, environmental protection (from dehydration and heating), and allows for the exocytosis of waste materials, which can be compared to similar biological behaviours found *In-vivo*. The bulk medium cells are grown in is a complex mixture of salts, amino acids, proteins, sugars and a few additional components that assist with pH balance ($NaHCO_3$) and as an indicator (phenol red). Two of the most common media used for this application are Eagle's minimum essential medium (EMEM) and Dulbecco's minimal essential medium (DMEM), the latter of which is an adaption to original EMEM recipe by increasing glucose concentration and amino acids, which presents issues for detection via electrochemical means. As such, the implementation of an electrode capable of accurately and reliably detecting and quantifying the concentration of H_2O_2 offers great advantage over conventional methods, such as chromatography or assays.

The research presented herein documents the characterisation of pad-printed commercially-available Prussian Blue doped Carbon ink to simply fabricate disposable electrodes, and their potential use for H_2O_2 quantification and monitoring was assessed. This emerging technology may be useful to help understand and study the role of H_2O_2 in cell culture and offer novel means to monitor stress induction/ fluctuation in bulk media in real-time.

2 Materials and Methods

2.1 Reagents and solutions

All chemicals used were of analytical/ cell culture grade and were used as received without any further purification (unless stated), and were acquired from Alfa Aesar (Haverhill, MO, USA), Sigma-Aldrich (St. Louis, MO, USA), Biowest (Rue de la Caille, Nuaillé, FR) and Lonza (Muenchensteinerstrasse, Basel, CH). All solutions were prepared with ultrapure water with resistivity of 18.2MΩ cm. Stock buffer solutions were prepared at x10 concentration and made to a working buffer concentration on the day of use. Commercially available carbon/ graphite and mediated pastes were used as the base for the carbon working and counter electrode printing inks (C2000802P2, C2070424P2 Gwent Electronics UK).

EMEM formulation was supplemented with heat-inactivated fetal calf serum (HIFC) (5% (v/v)), non-essential amino acids (NEAA) ((1% (v/v)) and 1% antibiotic-antimitotic (1%(v/v)) (herein referred to as complete media). DMEM formulation (high glucose) was supplemented with NEAA (1% (v/v)) and L-glutamine (2mM). Both formulations are considered 'complete' culture medium and are used routinely in cell culturing and molecular assays (CMEM and CDMEM, respectively).

Britton-Robin buffer (BRB) was prepared in-house; a x10 stock solution consisted of boric acid (0.4M), phosphoric acid (0.4M) and acetic acid (0.4M). A working BRB solution was created by diluting the stock solution 1/10 with ultrapure water, the pH was adjusted to a physiological pH of 7.4.

HeLa cells were acquired from the ECACC via Public Health England. Cells were routinely passaged 2-3 times a week, subject to growth and experimental requirements. Cells were maintained in a 37^{o}C, 5% CO_2 incubator and were passaged until the 15th subculture, at which point they were discarded, and a frozen stock revived and utilised. HeLa cells were maintained in CMEM at all times unless otherwise stated.

2.2 Molecular assays

2.2.0 Cell lysate preparation and quantification

Cells were lysed using a freeze-thaw method. Briefly, cells isolated in 1.5 mL microcentrifuge tubes were placed into a dewar of liquid nitrogen for ~30 seconds, removed and placed into a heat block at 40^{o}C for 5 minutes. This cycle was repeated 5 times to ensure cells were adequately lysed. Cells were centrifuged at 1.2X10^{4}g for 10min and the supernatant removed. 1mL of PBS was added to the cell lysate and cells were quantified by protein concentration via bicinchoninic acid assay (BCA). Briefly, 25µL of each sample was placed in a 96 well (in triplicate) along with a standard calibration range using bovine serum albumin. A BCA protein assay kit was purchased from ThermoFisher scientific (23225) and utilised as stated in the protocol. Cells were normalised using the lowest observed protein concentration (~300 and ~2000µg/mL for cell lysates and culture media, respectively; data not shown).

2.2.1 Ferrous ion oxidation Xylenol orange assay (FOX-2 assay) for lipid peroxide quantification

Method was adapted from Banerjee *et al.*, (2003) and Nourooz-Zadeh, (1999). Briefly, a final working solution (WS) consisted of 3.96mM butylated hydroxyl toluene, 247.5µM ammonium ferrous (II) sulfate, 123.76µM Xylenol orange, 98.81% methanol and 24.75% H_2SO_4. 90µL of sample was aliquoted into tubes in duplicate; 10µL of methanol was added to one tube and 10µL of triphenylphosphine (TPP, 10mM in methanol) in the other, with the second acting as a radical generator. Samples were vortexed for ~5s and left to incubate at room temperature for ~25min. 900µL of WS was added to each tube, vortexed and incubated at room temperature for ~25min. Samples were centrifuged at 1.2X10^{4}g for 10min and aliquoted into a 96-well plate in triplicate. Plates were read at 560nm.

2.2.2 Ampliflu red assay for peroxide quantification

Ampliflu red was dissolved in cell culture grade DMSO to a concentration of 10mM. The final concentration of WS consisted of 9.7mM, pH 7.4 PBS, 0.1mM Ampliflu red and 0.2U/mL Horseradish peroxidase. 50µL of samples were loaded into 96-well plates in triplicate; a calibration curve for H_2O_2 was constructed. 50µL of WS was added to each well, plates were incubated at room temperature for 30min and read at Ex545/Em590nm.

2.3 Instrumentation and software

All voltammetric and amperometric measurements were performed using a Metrohm autolab PGSTAT101 (Metrohm, Utrecht, Netherlands). Experiments were performed using a standard three-electrode system; a pad printed carbon working electrode (PPCE), an Ag/AgCl (3M NaCl, ALS) and a platinum wire (ALS, 99.95%). Results were computed in real-time using Autolab NOVA (version 2.0); all experiments were performed in a 10mL cell unless stated.

2.4 Pad-printed carbon electrode fabrication

Pad printed electrodes were prepared as previously detailed in McBeth *et al.*, (2018) . Briefly, the electrode was constructed using pad-printing methods. A commercial Prussian blue ink was acquired (Gwent group, C2070424P2, 42-43% solid constituents) and initially printed without further modification, (Figure 2).

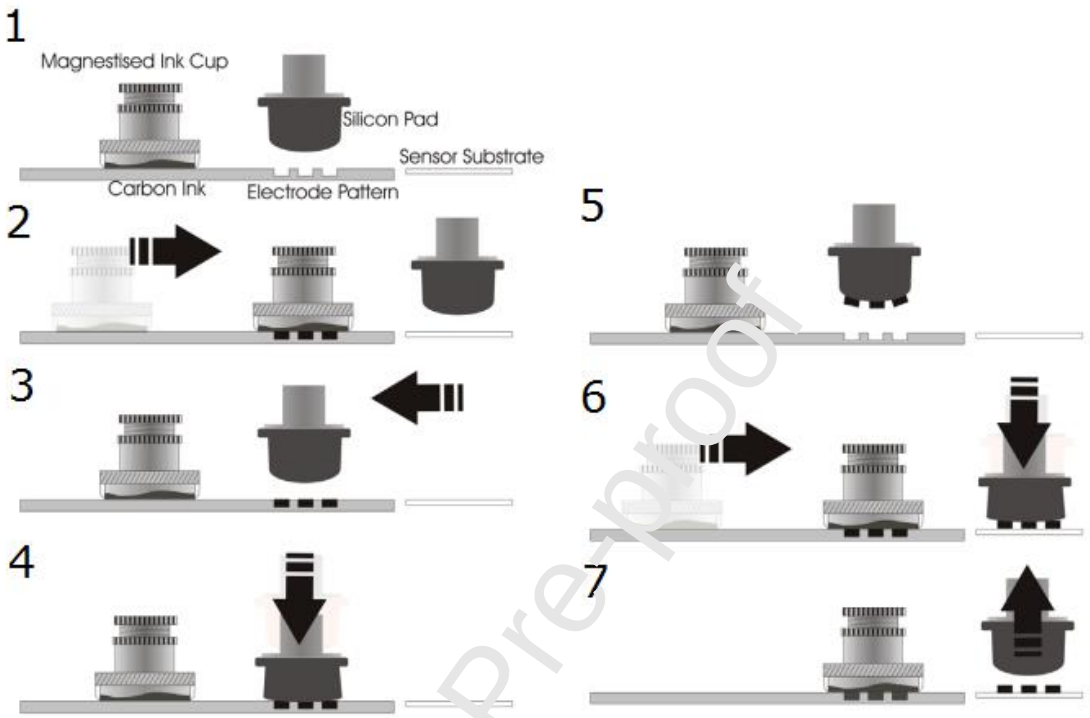

Figure 2 – The pad printing process, a carbon ink mixture is placed intro a magnetised cup and through an automated process is deposited into a steel cliché, collected via a silicon printing pad and is deposited on to electrode substrate. The presentation of the electrode is dictated by the design on the steel cliché.

The working electrode consisted of a deposition of 5 layers of PB-carbon graphite ink onto a 250-micron sheet of cellulose acetate, with an average depth of 5µm per layer. The working area of the pad-printed PB carbon electrode (PPPBCE) was 5.81mm^2 with an average diameter of 2.72mm. The working area was further defined by sealing the body of the electrode in-between a sheet of 80-micron laminating film (Ethylene-Vinyl Acetate inner, Polyethylene Terephthalate outer), by passing it through a 110^{o}C laminator 3 times in succession, shown in Figure 3. Electrodes were washed in deionised water and dried using nitrogen before use.

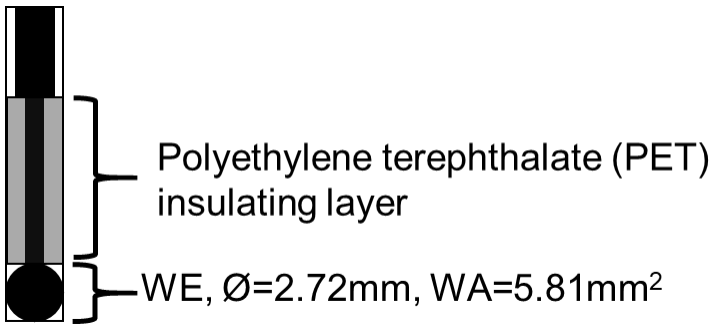

Figure 3 – Pad-printed WE composed of PB-carbon ink with PET insulating layer.

2.5 Sample preparation

2.5.1 Calibration and simulated samples

Samples were prepared using CMEM and 30% (W/W) H_2O_2. Samples were diluted to physiological concentrations of extracellular H_2O_2 (1-40µM) using CMEM[47].

2.5.2 Brefeldin A treated cells

HeLa cells were cultured at 37°C with 5% CO_2. Cells were seeded into flasks at a density of $1X10^5$ cells/ mL of CMEM, cultured overnight to a density of $2X10^5$ cells/ mL of CMEM in a 5% CO_2 incubator at 37°C. When cells were found to be ~50% confluent, media was removed and cells were washed with 0.1M PBS. EMEM was supplemented to desired concentrations of the hypoxia mimetic $CoCl_2 \cdot 6H_2O$ (final concentration 400-480µM) and endoplasmic reticulum stress inducer Brefeldin A (final concentration 0.01-5 µM). Following addition of stress inducer, samples were incubated for 18h at 37°C in 5% CO_2. Media was removed and immediately frozen at -80°C for further experimentation. For assays media was defrosted at room temperature and placed into a 37°C incubator with 5% CO_2 for 1h to allow culture pH to return to physiological levels. Samples were interrogated in a 10mL cell via a PPPBCE.

3. Results and Discussion

3.0 Molecular assay of media peroxides

Cell lysates and culture media was assessed to determine typical concentrations of aqueous and lipid peroxides found at the end of a 48 hr growth period (typical interval between media exchange[48]). As shown in Figure 4, cell lysate and culture media demonstrated similar concentrations of aqueous and lipid peroxides; the overall agreement between the two sampling methods suggests that culture media analysis can act as a good proxy for the more time consuming cell lysate analysis and provides the basis that minimally invasive analysis of the culture media – without formal sampling – is valuable. This demonstrates capacity for intracellular peroxides to be observed and monitored via bulk media peroxides using pad-printed electrodes without the need for end-point cell lysing.

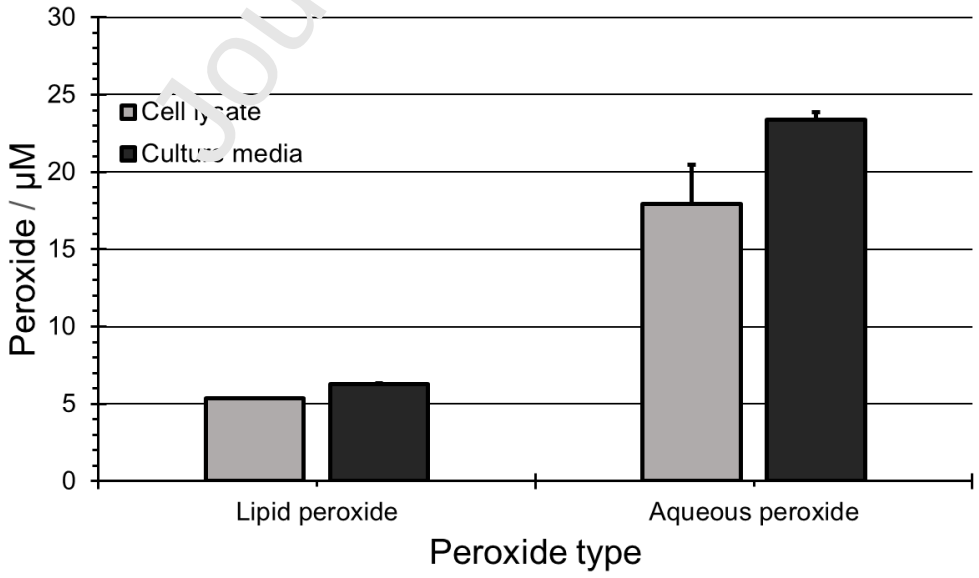

Figure 4 – Concentration of peroxides found in HeLa cell lysates and culture media using FOX-2 (lipid peroxides) assay and Ampliflu red (aqueous peroxides) (n=3).

As has been demonstrated, peroxides found in CMEM culture media and cell lysate has been quantified at a concentration of ~5-25µM, hence this represents the typical normal working range that is central to the proposed analytical tools – albeit having a detection range significantly above and below this would be of great importance for induced conditions and cellular behaviours that resulting in the change of H_2O_2 concentration.

3.1 Cyclic voltammetry

The behaviour of the pad-printed Prussian blue mediated ink was initially studied in three media of interest; Britton-Robinson Buffer, the simplest cell culture media (EMEM) and a more complex cell culture media (DMEM) to assess the anodic (E_{pa}) and cathodic peaks (E_{pc}) of the electrode in each media. Electrodes demonstrate an E_{pa} and E_{pc} peak at ~0.2 and 0.0V, respectively, in ~pH 7.5 EMEM and DMEM and 0.18 and -0.12V in pH 7.5 BRB, (Figure 5).

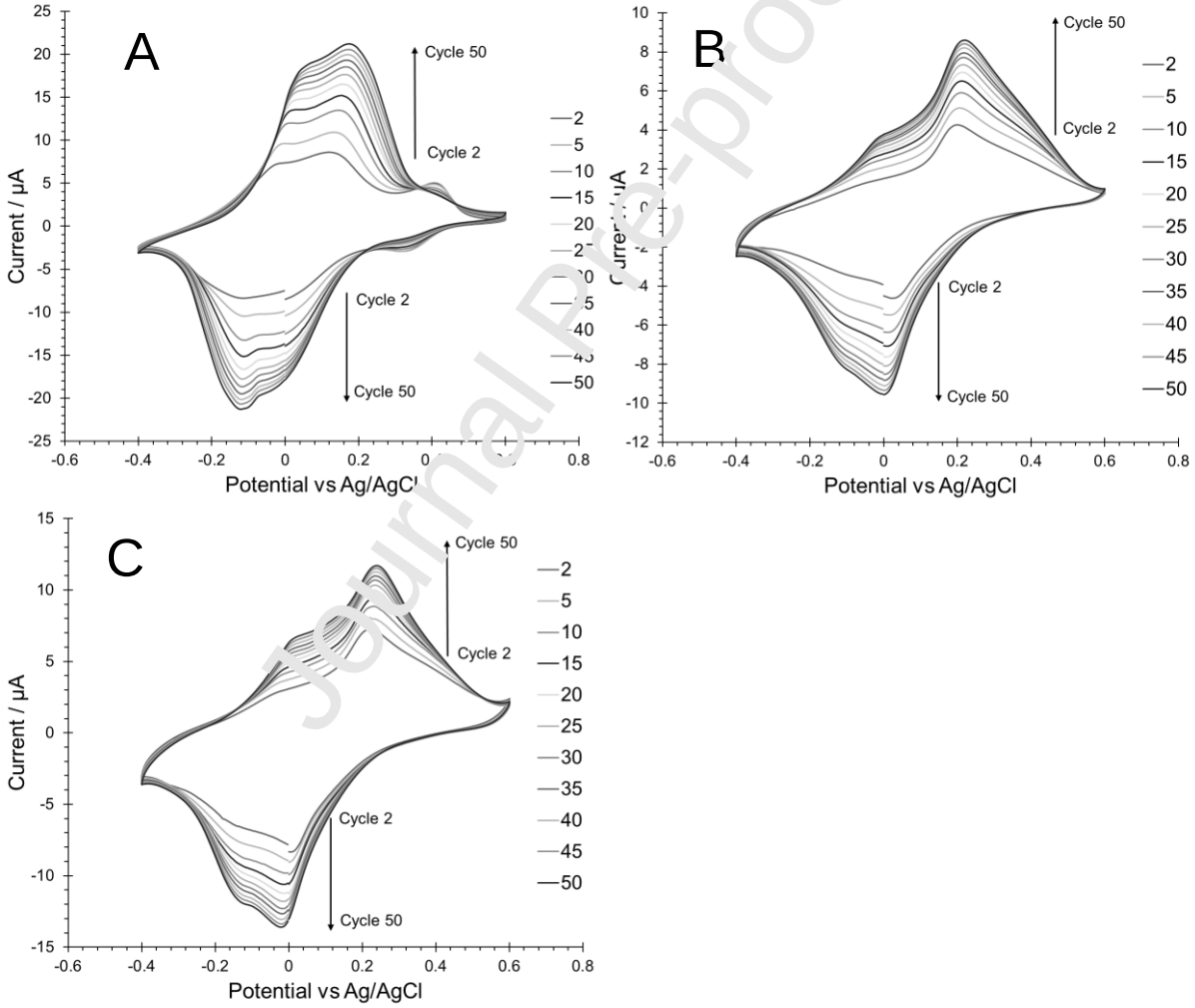

Figure 5 – CV progression of PPPBCEs in media. Sampling of every 5th cycle is represented for a total of 50 cycles for each media, **A)** BRB **B)** EMEM **C)** DMEM, scanned at 50mV/s vs Ag/AgCl (n=3)

Shown in Figure 5, the peak magnitudes increase with progressive cycles up to 50 cycles, attributed to cleaning of solvent residue and polymer from the active surface of the electrode

and equilibration resulting in a subsequent increase in redox peaks with each medium until a stable scan is achieved (~50th scan).

The surface of a pad-printed carbon electrode is not as faultless as that of a traditional GCE. Pad-printed electrodes present a rough, uneven texture compared to the smooth, polished surface of a GCE (as we have previously observed using AFM[49]), making exact determination of the contoured working area difficult. Because of this, each printed electrode can vary slightly in a batch and potentially present more variance between batches, however will benefit from having high surface area and presentation of more edge plane sites. This geometry may influence the diffusion coefficient of species due to the layering of Prussian blue ink layers. This will result in behaviours dissimilar to those observed in classic electrical double layer kinetics, which will be challenging to characterise due to the variation between each electrode. Using a Randles-sevcik plot, assessment of the slope of I_p vs scan rate$^{-1/2}$ was investigated, which demonstrated a linearity for I_{pa} and I_{pc} with R^2=0.9988 and 0.9879, respectively. This demonstrates conventional diffusion limitations at the surface of the electrode and eliminates potential notion for interfering redox events occurring at the electrode (Supplementary information Fig.1)

Demonstrated in Figure 6, an increase in I_{pc} can be observed at ~-0.1V with each 10µM addition of H_2O_2, also, a loss of pre and post faradaic current demonstrates a shift in current with a loss in the former and an increase in the latter. However, the current change in the defined E_{pa} occurring at ~0.3V does not express as much of a shift as the cathodic peak at ~-0.1V (as expected due to the reduction of H_2O_2 Figure 1), hence amperometric measurements will be explored at ~-0.1V to assess electrode sensitivity as they present the greatest current change at a defined potential upon addition of H_2O_2.

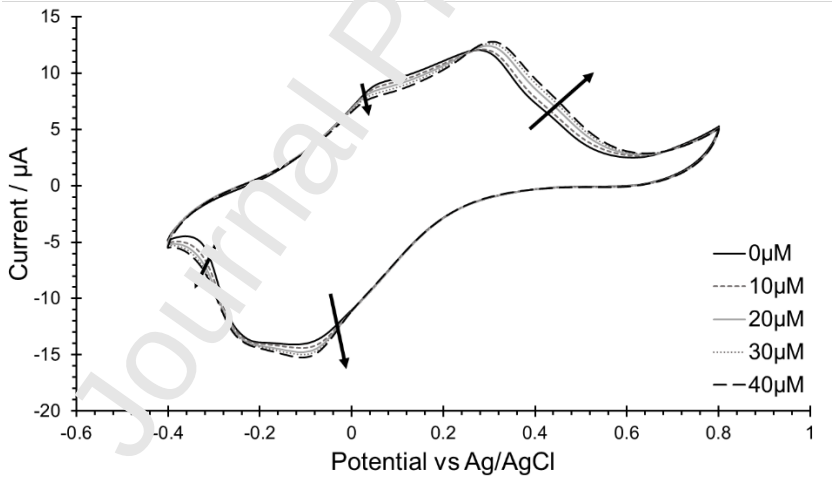

Figure 6 – CV progression of 10µM additions of H_2O_2 to EMEM media at PPPBCEs, scanned at 50mV/s vs Ag/AgCl (n=3)

3.2 Amperometric Measurements

Amperometry was utilised to identify the LOD, LOQ (supplementary information Eq1 and Eq2), and the linear range(s) for H_2O_2 sensing. A 10mL cell was utilised and was stirred between each subsequent addition of H_2O_2. Electrodes were initially cycled between -0.4 – 0.6V at 50mV/s for 50 cycles (Vs Ag/AgCl) and held at specific voltages for amperometric measurement. Electrodes were held at potential for 200s before spiking the BRB solution with 10mM H_2O_2 (final concentration of 10µM in cell), at ~60s intervals. -0.1V resulted in greatest increase (Supplementary information, Fig.2), without oxidative interference.

3.3 Calibration of Electrodes in media

To assess the calibration range of the PPPBCEs, testing was conducted in BRB to assess the baseline function of the electrode with limited potential interference from constituents found in cell culture media. To study biologically relevant concentrations of hydrogen peroxide, as demonstrated earlier, 1 and 5µM additions of hydrogen peroxide were used. Electrodes were cycled between -0.4 – 0.6V at 50mV/s for 50 cycles in 0.4M BRB vs Ag/AgCl. Before testing, BRB solution was replenished with fresh BRB and the electrodes rested for 200s at -0.1V to achieve a stable baseline before the introduction of exogenous H_2O_2 at 60s intervals for 15 spikes (Figure 7).

DMEM, a more complex aqueous medium with twice the concentration of amino acids compared to EMEM, was also explored due to its popularity of use in cell culture, especially for cells requiring richer mediums [50,51].

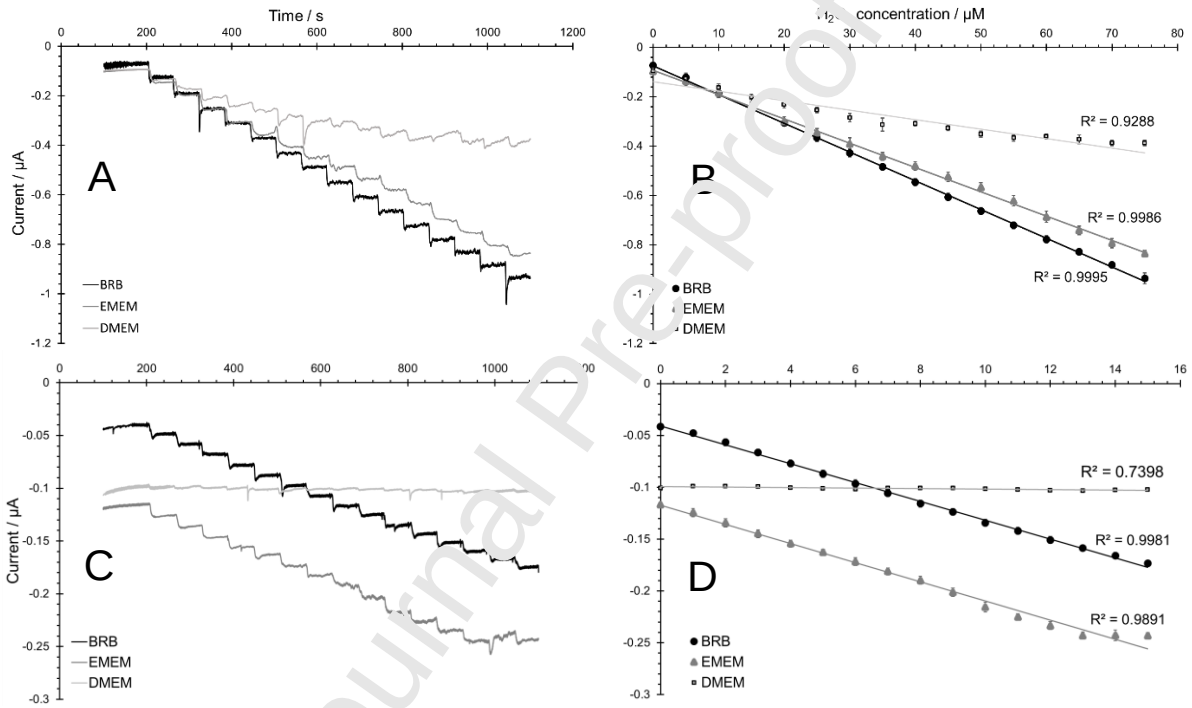

Figure 7 – Amperometric measurements of increasing concentrations of H_2O_2 in BRB, EMEM and DMEM at -0.1V vs Ag/AgCl. A – raw amperometric response to 5µM spikes of H_2O_2, B – Linear response to average value across time points for to 5µM spikes of H_2O_2, C – raw amperometric response to 1µM spikes of H_2O_2, and D - Linear response to average value across time points for to 1µM spikes of H_2O_2 (n=3).

For BRB and EMEM, increasing the concentration of H_2O_2 provided a predictable and linear response across both medium in 5µM additions; BRB: I_{pc} = -85.761[H_2O_2]/µM - 6.3388 (R^2 = 0.9995) and EMEM: I_{pc} = -101.31[H_2O_2]/µM-9.3445 (R^2 = 0.9986), was observed from 5-75 µM. Concentrations of 1-15µM in 1µM increments were also studied, providing similar results; BRB: I_{pc} = -109.83[H_2O_2]/µM-4.461 (R^2 = 0.9981), and EMEM: I_{pc} = -107[H_2O_2]/µM-12.459 (R^2 = 0.9891).

Calibrations were also performed in DMEM (Figure 6); a loss of linearity and steady loss of current with each addition is observed. The electroanalytical response is notably different; I_{pc} = -241.68[H_2O_2]/µM-30.977 (R^2 = 0.9288) across larger concentrations (5-75µM, 5µM

increments), and an I_{pc} = -3110.5[H_2O_2]/µM-306.99 (R^2 = 0.7398) for the lower concentrations (1-15µM, 1µM increments).

As such, the electrode demonstrates an ability to work effectively in BRB and EMEM, however, DMEM does not hold a stable current over time and demonstrates a slow return towards baseline with each addition of H_2O_2. This instability is possibly due to the antioxidant properties present in the culture medium, which is not as prevalent in EMEM, potentially due to the lower concentration of constituents.

Calibration in the presence of serum– spiked cell culture media

To determine the electrode capacity to function in the presence of serum, EMEM was supplemented with 5% (V/V) HIFC serum (to form CMEM) (Figure 8). Due to the fluctuations in baseline current, the resting period was extended until a stable baseline current was maintained for a minimum of 100s. Following an extended stabilisation period (500s), H_2O_2 was added to the media, providing a similar, and reliable, linear agreement [I_{pc} = -0.0099[H_2O_2]/ µM -0.0678, R^2=0.9997) across an extended H_2O_2 range of 1-200µM.

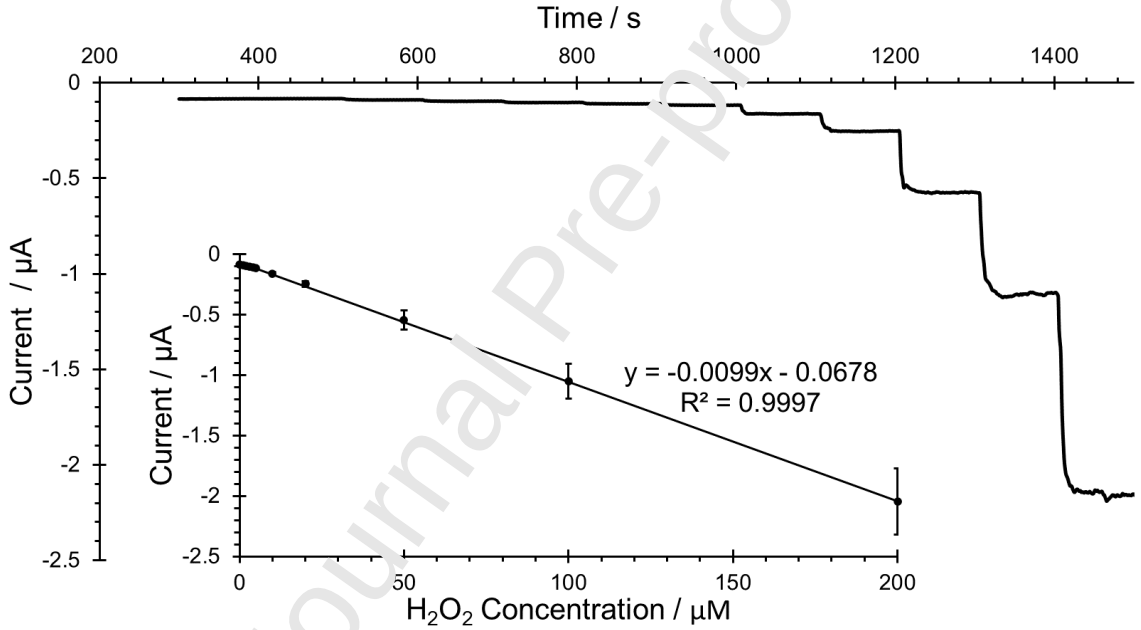

Figure 8 – Amperometric measurement of increasing concentrations of H_2O_2 in CMEM (5% HIFC) across a 0-200µM range, (n=3)

PPPBCEs demonstrated capacity to detect H_2O_2 in CMEM (5%) with high sensitivity. Two ranges were explored, 1-10 and 1-200µM. Electrodes demonstrated reliable linearity from 1-200µM, I_{pc} = -101.32[H_2O_2]/µM-6.8531 (R^2 = 0.9997), LOD and LOQ were determined using the correlation I_{pc} = -130.69[H_2O_2]/µM-10.48 (R^2 = 0.9948) as attained from the 1-10µM range. LOD was determined to be 0.5µM and LOQ to be 0.9µM in CMEM.

Table 2 – Comparison of H_2O_2 sensing capacity of PPPBCE in tested mediums

Medium	Linear range	LOD	LOQ	Sensitivity (µA/µM/mm^2)
BRB	0.41-200µM	0.41µM	1.55µM	-22.543
EMEM	0.38-200µM	0.38µM	1.31µM	-23.562
DMEM	9.19-200µM	9.19 µM	12.09 µM	-674.061
CMEM	0.5-200µM	0.5µM	0.9µM	-27.844

Demonstrated in Table 2, the PPPBCE's demonstrate capacity to detect H_2O_2 at concentrations relevant to cell culture media, commonly 10-80µM, and lower. As can be observed, LOD and LOQ for mediums BRB, EMEM and CMEM are within a ~0.5µM range, however DMEM demonstrates ~x10 increase, comparatively. As previously mentioned, concentration of media constituents varies, with a variation in amino acids, bicarbonate, glucose and vitamins; DMEM is a much 'richer' medium containing increased concentrations of aforementioned constituents. This increase in concentration presents increased potential for limiting of electron transfer and reducing peroxide species innately, which is evident in Figure 7.

Electrodes demonstrated no signs of fouling at the electrode surface and a lower LOQ in media with serum. As previously stated, the zeolitic structure of PB inhibits the passage of larger molecules, reducing the potential of fouling/ adsorption within the carbon electrode matrix. This demonstrates that the electrode does not require a protective coating to protect from biofouling, and as PB is not water soluble, it does not need additional binding/ cross-linking agents to prevent leaching into the cell media or cell monolayer.

These results, even without further electrode modifications or protective coatings, are comparable to those reported in the literature (Table 3).

Table 3 – Comparison of various carbon electrodes utilising PB as a mediator of H_2O_2

Electrode	LOD	LOQ	Linear range	References
Screen printed carbon	0.4µM	-	0.4 -100µM	[24]
Inkjet-printed carbon	20µM	-	20 - 700µM	[43]
Screen printed graphite	1µM	-	1 - 500µM	[39]
Carbon paste	2.5µM	-	2.5 - 2000µM	[40]
Screen printed carbon	1.3µM	-	-	[52]
Pad-printed carbon	0.5µM (CMEM)	0.9µM (CMEM)	0.9- 200µM (CMEM)	This study

To understand the potential application of these electrodes even further, other experimental considerations commonly encountered in cell culture were studied: pH, temperature and reusability.

3.4 Effect of pH

EMEM, and most growth media, maintain pH via a $NaHCO_3$/ CO_2 buffering system within a culture incubator. Culture media exposed to external environments exhibit a pH shift occurs towards basic pH due to the reduction in CO_2 concentration. The shift in pH slows at a pH of 8.5 with little change observable over a 30min period in a normal temperature and pressure (NTP) environment.

Buffering EMEM at concentrations between a pH of 6-9 does not affect the ΔE_{pa} of the cyclic voltammogram for PPPBCEs (Figure 9). This grants detection of H_2O_2 at a variety of physiological pH concentrations without the need to adjust media pH prior to amperometric measurement; similar results were reported by Ricci *et al.*, (2003).O'Halloran, Pravda and Guilbault, (2001) states a change pH is expected in more basic media due to the hydrolysis of Fe^{3+} to Fe(OH), resulting in the loss of sensitivity. However, as we have demonstrated with the PPPBCE, sensitivity is retained at a pH of 6 to 9, this allows the electrode to be utilised efficiently without having to recalibrate the electrode for shifts in pH.

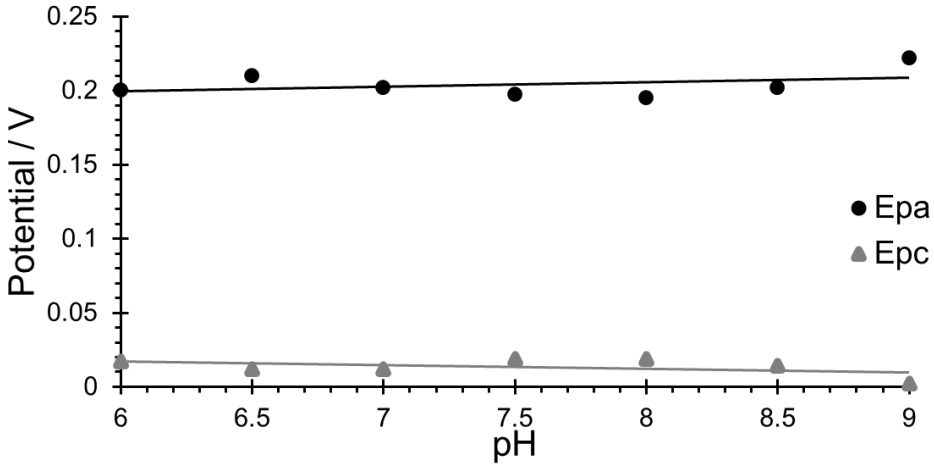

Figure 9 – Effect of pH on ΔE_p – pH range of 6-9 was assessed in 0.5 pH intervals, mean (SD) = E_{pa} 0.204(±0.009), E_{pc} 0.014(±0.006) vs Ag/AgCl (n=3)

3.5 Interference studies

To assess potential for interference from known antioxidants and amino acids, such as uric acid, ascorbic acid and cysteine, electrodes were held at -0.1V and two concentrations of each were utilised (Figure 10A). The range explored consisted of values previously specified in literature[53,54]; however due to a potential discrepancy with uric acid, values in excess of physiological standards were also assessed (Figure 10B).

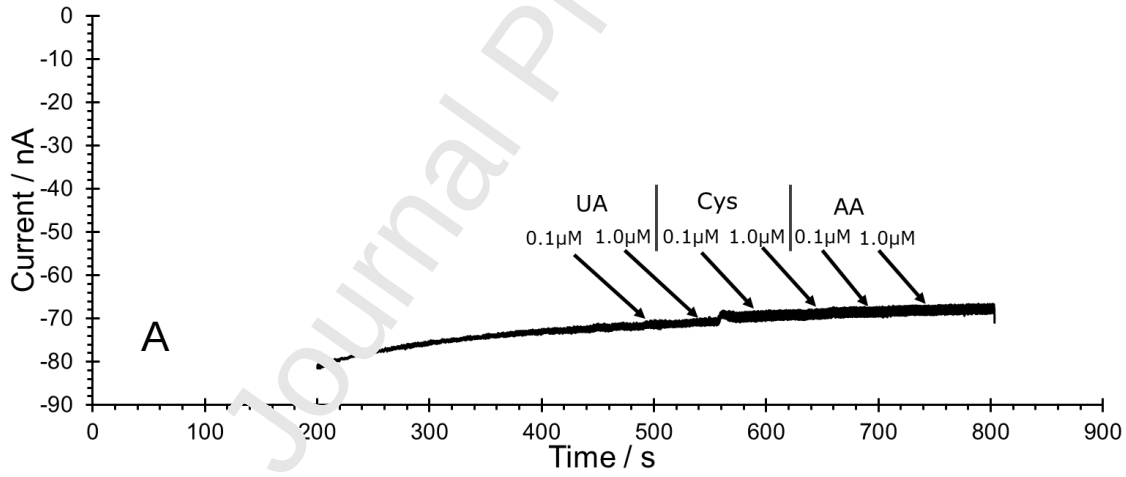

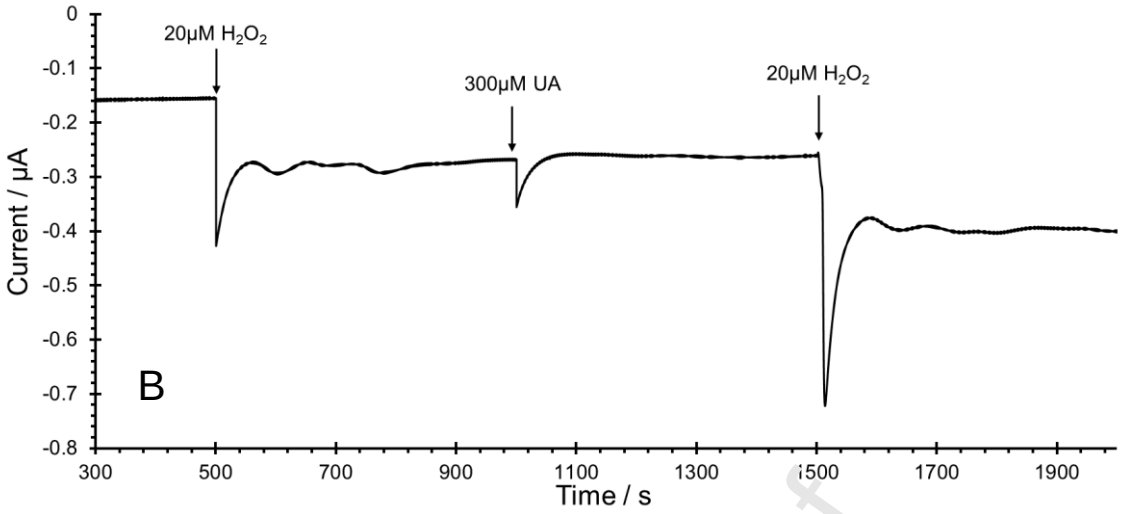

Figure 10A - Amperogram of potential interfering molecules - PPPBCE baseline with the addition of 0.1 and 1.0μM of uric acid, cysteine and ascorbic acid in 50s intervals. Note that baseline does not plateau but drifts towards 0.0V at a rate of 11.75pA/s from 500s onwards. **B** - 20μM concentrations of hydrogen peroxide spiked at 200s intervals in 10μL volumes. 300μM uric acid was spiked 100s after hydrogen peroxide addition to assess potential as an interfering molecule.

Initial experimentation demonstrated potential for interference from <1.0μM concentrations of uric acid, and no observable interference from ascorbic acid or cysteine. In regards to cell culture, urate is not a common target analyte due to its low concentration; however, in human and bovine sera, uric acid is found in a much greater concentration.

Due to the potential uses of this electrode both in cull media and other biological mediums, testing of the electrode in a medium containing serum levels of uric acid (AU) was also assessed, shown in figure 10B. Serum levels of UA are found to commonly be between 200-400μM[55], so a mid-point of 300μM was assessed. A dip was experienced on the introduction of UA to the culture medium but quickly returned to values previously shown, this dip was likely due to the movement of fluid within the medium upon introduction. The further introduction of H_2O_2 demonstrated capacity to influence current in the presence of serum levels of uric acid

3.6 Reusability

Electrodes were assessed for their potential to be reused and for long-term use for which they must demonstrate reliability to accurately monitor changes in H_2O_2 concentration. Electrodes were cycled in CMEM for 50 cycles at 50mV/s, media was exchanged with fresh CMEM and electrodes were assessed for reusability using amperometry. A rate of 1/200ms was utilised and a baseline established at -0.1V vs Ag/AgCl. At the 200s interval, media was spiked with 20μM H_2O_2 and observed for 200s. Electrodes were removed from the media and washed using ddH_2O. Media was replaced with CMEM, electrodes were placed back into the medium and observed for a further 200s to establish a new baseline. At 600s, media was again spiked with 20μM H_2O_2 and observed for 200s, shown in Figure 11.

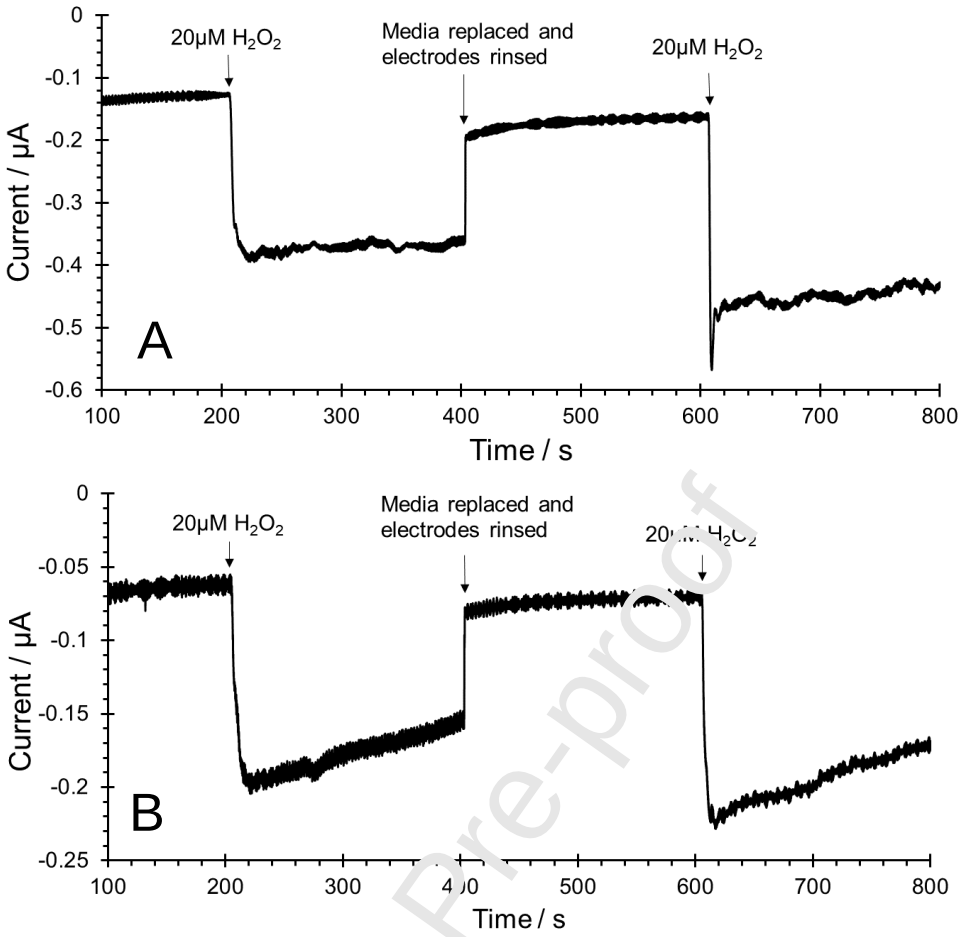

Figure 11 – Amperograms showing baseline (100-200s), 20μM spike (200-400s), media change and electrode rinse (400s) followed by repeating the baseline measurement (400-600s) and spiking with H_2O_2 (600-800s) in **A)** CMEM **B)** DMEM vs Ag/AgCl (n=3).

Separate spiking of the medium with H_2O_2 demonstrates similarities in initial change of current with a shift of ~-0.222μA and -0.114μA in CMEM and DMEM, respectively. After rinsing in ddH_2O, the current increased, though not completely to baseline, and displayed an increase in the current drop in response to additional H_2O_2.

As can be observed in the DMEM amperogram (Figure 11B), background is significantly greater than that of samples cultured in CMEM, however this is potentially due to electrode variance, hence the observed lower current range. The electrode does demonstrate similar behaviours as observed in electrode calibration studies (Figure 7), with the current gradually returning to baseline after the introduction of H_2O_2, further supporting the reducing influence of DMEM media.

Therefore, the basic electrode design demonstrates apt potential for the long-term monitoring of H_2O_2 in a cell culture media. Future work needs to consider the longitudinal reliability, fouling potential and retained sensitivity. However, the work shown here demonstrates the PPPBCEs have the capacity to monitor sub-micromolar concentrations of H_2O_2 with a wide linear range in complete media (Table 2). These electrodes can therefore be considered an accurate means of measuring observed concentrations of H_2O_2 in cell culture (Figure 4).

As the use of these PPPBCEs have been well-characterised, a novel concept to explore is the potential for H_2O_2 concentration to fluctuate in cell culture media; literature commonly focuses on the increases in I_p with an increase in H_2O_2 concentration, few explore the reaction kinetics of H_2O_2 elimination.
An unexplored use of PPPBCEs in cell culture for the sensing of H_2O_2 is monitoring the elimination of H_2O_2 from media through a secondary mediator. The introduction of double mediators can greatly influence the concentration of various biomarkers in culture media, and can inhibit the accumulation and action of several biomarkers, such as H_2O_2. As such, monitoring the rate of these reactions can be observed using PPPBCEs by observing the reduction of current with the addition of H_2O_2 to various mediators.

3.6 $CoCl_2$ influence on PB reduction

$CoCl_2$ was assessed for two mechanisms; initially as a hypoxia mimetic inducer of hypoxia-inducible factor-1α[56–58], which can induce various pathologies via oxidative stress induction[59]. However, as a transition metal it is capable of catalysing Fenton-like processes converting H_2O_2 into the more reactive hydroxyl radical. Hence, $CoCl_2$ induces oxidative stress in cellular systems by accumulating HIF-1α proteins (leading to mitochondrial dysfunction) and act as a catalyst for hydroxyl radicals' ions in the presence of peroxides[60–62].
HeLa cells were exposed to $CoCl_2$:$6H_2O$ in CMEM across a range of 260-700µM and viability was assessed via MTT assay (supporting information Fig.3), HeLa cells demonstrate a significant loss in viability between 400-460µM.

It is well established that Cobalt (II) is oxidised to Cobalt (III) in the presence of H_2O_2 resulting in the creation of hydroxyl radicals[63]. To potentially observe the rate at which this reaction can occur, hydrogen peroxide reduction was assessed in the presence of $CoCl_2$.

Culture media spiked with $CoCl_2$ was subject to increasing concentrations of H_2O_2 to test the initial response and whether the degradation / consumption of H_2O_2 could be studied using this system. Shown in Figure 12A, after each spike H_2O_2, the current returns to baseline, but requires longer to do so as concentration increases (Figure 12B). Concentrations of H_2O_2 <10µM demonstrate decreased current as time proceeds, potentially indicating such low concentrations of H_2O_2 are reduced before reaching the electrode surface.

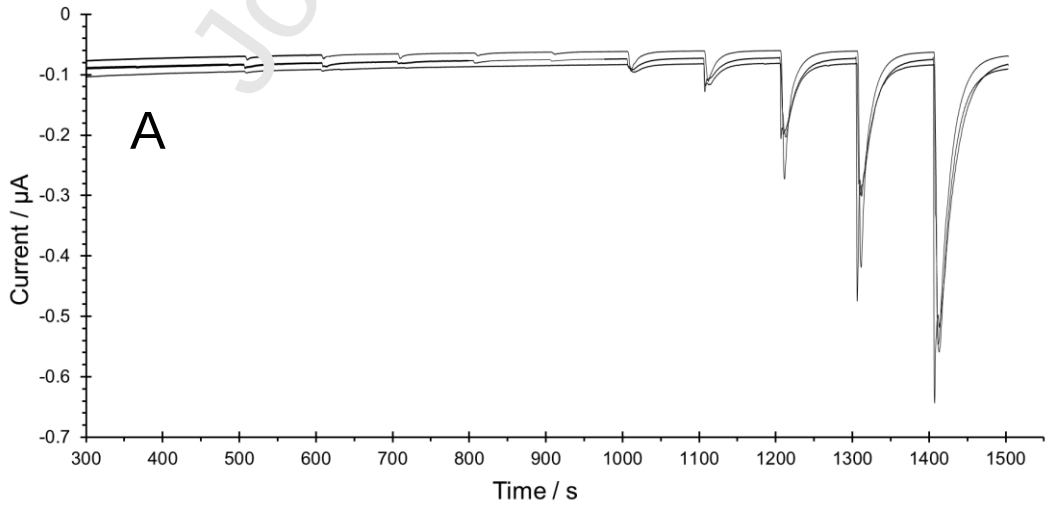

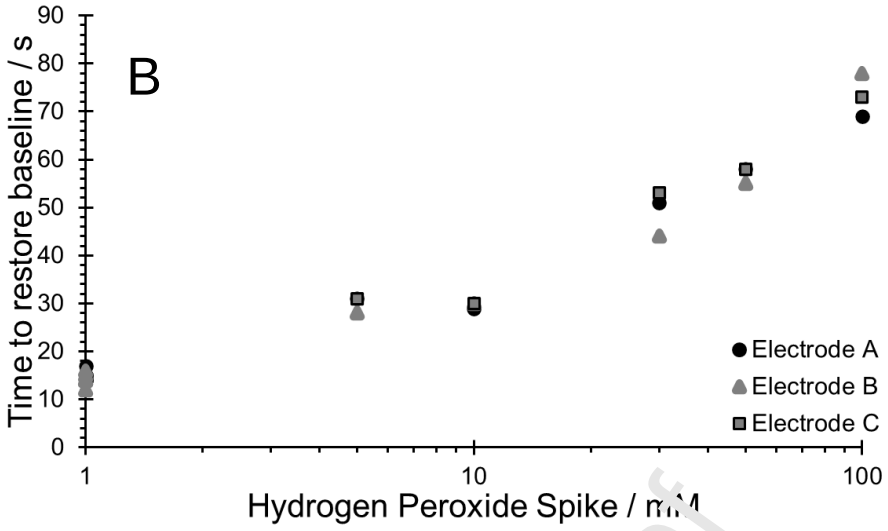

Figure 12 – **A**. H_2O_2 spike response in EMEM with 400µM $CoCl_2$ for 3 separate electrodes. **B.** Time to return to baseline for H_2O_2 spiked EMEM with 400µM $CoCl_2$ for 3 separate electrodes. H_2O_2 concentrations 1, 2, 3, 4, 5, 10, 20, 50, 100, and 200 µM (cumulative).

The compound $CoCl_2$ is known to induce ROS by acting as a hypoxia mimetic, though literature demonstrates pathological variance compared to physical/ environmental hypoxia. While alternative hypoxia mimetics exist, such as desferrioxamine, literature highlights the antioxidant properties of the compound due its iron chelating capacity, which may interfere with the generation of peroxide molecules[58,64,65].

There is an almost immediate return to baseline current across 1-10 µM H_2O_2 spiking, though higher concentrations require longer (~100s for 200 µM), they too return to similar current values as baseline. This is further supported in literature, $CoCl_2$ complexes are well documented for their capacity to be substituted and form ligands with amino acids[61,66] or act as direct site for H_2O_2 decomposition, leading to the generation of $O_2^{-\bullet}$[67], and for Fenton-like processes.

Therefore, the presented sensing approach may also allow *in-vivo* studies of peroxide reduction through Fenton-like processes, as shown for Cobalt, which allow for reaction kinetics to be further explored in similar systems.

5.4 Conclusion

The research presented here outlines the simple fabrication and characterisation of a pad-printed Prussian blue carbon electrode which, without further modification, has proven capable of reliably quantifying hydrogen peroxide in buffered solutions and cell culture media.

Electrodes demonstrated a LOD of 0.41µM in BRB, 0.38µM in EMEM and 9.19µM DMEM for hydrogen peroxide sensing, and LOQ of 1.55µM, 1.31µM and 12.09µM in BRB, EMEM and DMEM, respectively. Electrodes were tested in a conventionally supplemented cell culture medium, CMEM (5% serum content), and still demonstrated an LOD of 0.5µM and an LOQ of 0.9µM. Electrodes demonstrate capacity to detect H_2O_2 with a linear range of 1-200µM in CMEM, with a correlation of $y = -0.0134x - 0.3351$ (R^2 =0.9988), which is comparable to similar electrodes in literature.

The interaction between H_2O_2 and $CoCl_2$ was also explored; electrodes demonstrated the rate of H_2O_2 neutralisation in the presence of $CoCl_2$. This mechanism could be utilised to

assess the potential for other compound interactions with H_2O_2 reduction in similar complex environments.

Overall, these proof of concept results illustrate the potential applicability of novel, simple, pad-printed Prussian blue electrodes to monitor peroxide in-situ in bulk cell culture environments. The ability to print small, versatile and robust electrodes for cell culture monitoring would offer a novel tool and provide a step-change in the available technologies for research to monitor chemical changes in-situ and without sample preparation.

References

1 D. R. Gough and T. G. Cotter, *Cell Death Dis*, 2011, **2**, e213.
2 E. A. Veal, A. M. Day and B. A. Morgan, *Mol. Cell*, 2007, **26**, 1–14.
3 M. Giorgio, M. Trinei, E. Migliaccio and P. G. Pelicci, *Nat Rev Mol Cell Biol*, 2007, **8**, 722–728.
4 G. Waris and H. Ahsan, *J. Carcinog.*, 2006, **5**, 14.
5 C. Calas-Blanchard, G. Catanante and T. Noguer, *Electroanalysis*, 2014, **26**, 1277–1286.
6 R. Pauliukaite, S. B. Hočevar, E. A. Hutton and B. Ogorevc, *Electroanalysis*, 2008, **20**, 47–53.
7 B. Çeken, M. Kandaz and A. Koca, *J. Porphyr. Phthalocyanines*, 2012, **16**, 380–389.
8 M. Holzinger, A. Le Goff and S. Cosnier, *Front. Chem.*, 2014, **2**, 63.
9 V. Pifferi, G. Cappelletti, C. Di Bari, D. Meroni, F. Spadavecchia and L. Falciola, *Electrochim. Acta*, 2014, **146**, 403–410.
10 C. Boero, S. Carrara and G. De Micheli, in *Research in Microelectronics and Electronics, 2009. PRIME 2009. Ph. D.*, IEEE, 2009, pp. 72–75.
11 C. Boero, M. A. Casulli, J. Olivo, L. Foglia, E. Orso, M. Mazza, S. Carrara and G. De Micheli, *Biosens. Bioelectron.*, 2014, **61**, 251–259.
12 M. Asif, A. Aziz, Z. Wang, G. Ashraf, J. Wang, H. Luo, X. Chen, F. Xiao and H. Liu, *Anal. Chem.*, 2019, **91**, 3912–3920.
13 M. A. Kamyabi and N. Hajari, *J. Braz. Chem. Soc.*, 2017, **28**, 808–818.
14 C. Karuppiah, S. Palanisamy, S.-M. Chen, V. Veeramani and P. Periakaruppan, *Sensors Actuators B Chem.*, 2014, **196**, 450–456.
15 C. Batchelor-McAuley, Y. Du, G. G. Wildgoose and R. G. Compton, *Sensors Actuators B Chem.*, 2008, **135**, 230–235.
16 M. Asif, H. Liu, A. Aziz, H. Wang, Z. Wang and M. Ajmal, *Biosens. Bioelectron.*, 2017, **97**, 352–359.
17 A. V Mokrushina, M. Heim, E. E. Karyakina, A. Kuhn and A. A. Karyakin, *Electrochem. commun.*, 2013, **28**, 78–80.
18 J. Ping, J. Wu, K. Fan and Y. Ying, *Food Chem.*, 2011, **126**, 2005–2009.
19 X.-G. Li, M.-R. Huang, W. Duan and Y.-L. Yang, *Chem. Rev.*, 2002, **102**, 2925–3030.
20 B. Haghighi, H. Hamidi and L. Gorton, *Sensors Actuators B Chem.*, 2010, **147**, 270–276.
21 J. Zhao, P. Yue, S. Tricard, T. Pang, Y. Yang and J. Fang, *Sensors Actuators B Chem.*, 2017, **251**, 706–712.
22 J. P. Hart, A. Crew, E. Crouch, K. C. Honeychurch and R. M. Pemberton, *Anal. Lett.*, 2004, **37**, 789–830.
23 H. Byrd, B. E. Chapman and C. L. Talley, *J. Chem. Educ.*, 2013, **90**, 775–777.
24 M. P. O'Halloran, M. Pravda and G. G. Guilbault, *Talanta*, 2001, **55**, 605–611.
25 E. Nossol and A. J. G. Zarbin, *J. Mater. Chem.*, 2012, **22**, 1824–1833.
26 M. Raicopol, A. Prună, C. Damian and L. Pilan, *Nanoscale Res. Lett.*, 2013, **8**, 316.
27 A. M. Farah, N. D. Shooto, F. T. Thema, J. S. Modise and E. D. Dikio, *Int. J. Electrochem. Sci.*, 2012, **7**, 4302–4313.
28 P. C. Pandey and A. K. Pandey, *Electrochim. Acta*, 2013, **87**, 1–8.
29 A. A. Karyakin, E. A. Puganova, I. A. Budashov, I. N. Kurochkin, E. E. Karyakina, V. A. Levchenko, V. N. Matveyenko and S. D. Varfolomeyev, *Anal. Chem.*, 2004, **76**, 474–478.
30 A. Malinauskas, R. Araminait, G. Mickevičiūt and R. Garjonyt, *Mater. Sci. Eng. C*, 2004, **24**, 513–519.
31 S. Han, Y. Chen, R. Pang, P. Wan and M. Fan, *Ind. Eng. Chem. Res.*, 2007, **46**, 6847–6851.
32 B. Haghighi, S. Varma, F. M. A. Sh, Y. Yigzaw and L. Gorton, *Talanta*, 2004, **64**, 3–12.

33 J. Wang, Y. Wang, M. Cui, S. Xu and X. Luo, *Microchim. Acta*, 2017, **184**, 483–489.
34 Q. Sheng, D. Zhang, Q. Wu, J. Zheng and H. Tang, *Anal. Methods*, 2015, **7**, 6896–6903.
35 Z. Cheng, Q. Shen, H. Yu, D. Han, F. Zhong and Y. Yang, *Microchim. Acta*, 2017, **184**, 4587–4595.
36 T. S. T. Balamurugan, V. Mani, C. C. Hsieh, S. T. Huang, T. K. Peng and H. Y. Lin, *Sensors Actuators, B Chem.*, 2018, **257**, 220–227.
37 P. Salazar, M. Martín, R. Roche, R. D. O'Neill and J. L. González-Mora, *Electrochim. Acta*, 2010, **55**, 6476–6484.
38 S. Cinti, F. Arduini, D. Moscone, G. Palleschi and A. J. Killard, *Sensors (Basel).*, 2014, **14**, 14222–14234.
39 F. Ricci, A. Amine, G. Palleschi and D. Moscone, *Biosens. Bioelectron.*, 2003, **18**, 165–174.
40 D. Moscone, D. D'ottavi, D. Compagnone, G. Palleschi and A. Amine, *Anal. Chem.*, 2001, **73**, 2529–2535.
41 S. Husmann, E. Nossol and A. J. G. Zarbin, *Sensors Actuators B Chem.*, 2014, **192**, 782–790.
42 E. K. Varadharaj and N. Jampana, *ECS J. Solid State Sci. Technol.*, 2015, **4**, S3077–S3082.
43 J.-Y. Hu, Y.-P. Lin and Y.-C. Liao, *Anal. Sci.*, 2012, **28**, 135.
44 D. Banerjee, U. K. Madhusoodanan, M. Sharanabasappa, S. Ghosh and J. Jacob, *Clin. Chim. Acta*, 2003, **337**, 147–152.
45 J. Nourooz-Zadeh, in *Methods in enzymology*, Academic Press, 1999, vol. Volume 300, pp. 58–62.
46 C. McBeth, R. Al Dughaishi, A. Paterson and D. Sharp, *Biosens. Bioelectron.*, 2018, **113**, 46–51.
47 B. Halliwell and M. Whiteman, *Br. J. Pharmacol.*, 2004, **142**, 231–255.
48 C. D. Helgason and C. Miller, *Basic Cell Culture Protocols*, 2004.
49 D. Sharp, *Biosens. Bioelectron.*, 2013, **50**, 399–405.
50 Z. Yang and H.-R. Xiong, in *Biomedical Tissue Culture*, InTech, 2012.
51 M. Arora, *Mater methods*, 2013, **3**, 175.
52 Z.-H. Li, H. Guedri, B. Viguier, S.-G. Sun and J.-L. Marty, *Sensors*, 2013, **13**, 5028–5039.
53 B. Thakur and S. N. Sawant, *Chempluschem*, 2013, **78**, 166–174.
54 B. Pollack, S. Holmberg, D. George, I. Tran, M. Madou and M. Ghazinejad, *Sensors*, 2017, **17**, 2407.
55 M. K. Kutzing and B. L. Firestein, *J. Pharmacol. Exp. Ther.*, 2008, **324**, 1–7.
56 M. S. Al Okail, *J. Saudi Chem. Soc.*, 2010, **14**, 197–201.
57 G. Chachami, G. Simos, A. Hatziefthimiou, S. Bonanou, P.-A. Molyvdas and E. Paraskeva, *Am J Respir Cell Mol Biol*, 2004, **31**, 544–551.
58 A. Triantafyllou, P. Liakos, A. Tsakalof, E. Georgatsou, G. Simos and S. Bonanou, *Free Radic. Res.*, 2006, **40**, 847–856.
59 D. E. B. Swinson and K. J. O'Byrne, *Clin. Lung Cancer*, 2006, **7**, 250–256.
60 M. Garoui el, H. Fetoui, F. Ayadi Makni, T. Boudawara and N. Zeghal, *Exp Toxicol Pathol*, 2011, **63**, 9–15.
61 P. J. Das, A. Das and A. Baruah, .
62 M. Guo, L. P. Song, Y. Jiang, W. Liu, Y. Yu and G. Q. Chen, *Apoptosis*, 2006, **11**, 67–77.
63 M. Valko, Cj. Rhodes, J. Moncol, M. M. Izakovic and M. Mazur, *Chem. Biol. Interact.*, 2006, **160**, 1–40.
64 A. Sanjuán-Pla, A. M. Cervera, N. Apostolova, R. Garcia-Bou, V. M. Víctor, M. P. Murphy and K. J. McCreath, *FEBS Lett.*, 2005, **579**, 2669–2674.
65 E. Shimoni, R. Armon and I. Neeman, *J. Am. Oil Chem. Soc.*, 1994, **71**, 641–644.
66 C. M. Wallen, L. Palatinus, J. Bacsa and C. C. Scarborough, *Angew. Chemie*, 2016, **128**, 12081–12085.

67 P. M. Hanna, M. B. Kadiiska and R. P. Mason, *Chem. Res. Toxicol.*, 1992, **5**, 109–115.

Credit author statement

Craig McBeth, Andrew Paterson, and Duncan Sharp were responsible for the conceptualisation of the work undertaken.

Craig McBeth, Andrew Paterson, and Duncan Sharp were responsible for the methodology of the work undertaken. Andrew Paterson is an expert of cell culture who supported Craig McBeth in the method design and implementation of cell-based investigation. Duncan Sharp is an expert in electrochemistry and carbon electrode fabrication who supported Craig Mcbeth in design and fabrication of electrodes and electrochemical experiment design and interrogation.

Craig McBeth was responsible for the validation of the work undertaken

Craig McBeth was responsible for the investigation of the work undertaken

Craig McBeth was responsible for the original draft of the work undertaken

Craig McBeth, Andrew Paterson, Duncan Sharp were responsible for the reviewing and editing of the work undertaken.

Craig McBeth and Duncan Sharp were responsible for the creation of visualisation data of the work undertaken

Andrew Paterson and Duncan Sharp were responsible for the supervision of the work undertaken

Leeds Beckett University was responsible for the funding of materials, resources, and equipment for the work undertaken.

We have no conflicts of interest with other groups and are happy for any referees to review the paper. None of the work in the paper has been published and it is not being considered for publication elsewhere. I can be contacted by email (Craig.McBeth@warwick.ac.uk).

Highlights

- Prussian blue mediated printed carbon electrodes allows *in-situ* determination of peroxide
- Pad-printed Prussian blue electrodes demonstrate capacity to monitor both the exogenous production of peroxide and elimination via Fenton-like processes.
- Capable of linearly detecting peroxide found below, across and above cellular concentrations of peroxide.
- Constructed electrodes proven capable of reliably determining peroxide in complex cell culture media